2019-05

GRAVEL BEACH CROSS- AND ALONGSHORE RESPONSE TO AN EXTREME EVENT: BEACH LENGTH AND HEADLAND PROXIMITY CONTROLS

McCarroll, Jak

10.1142/9789811204487_0234
Coastal Sediments 2019
WORLD SCIENTIFIC

McCarroll et al. 2019. Author's version of article in Proceedings of Coastal Sediments 2019

Gravel beach cross- and alongshore response to an extreme event: Beach length and headland proximity controls

R. JAK MCCARROLL[1], GERD MASSELINK[1], MARK WIGGINS[1], TIM SCOTT[1], OLIVER BILLSON[1,2], DANIEL CONLEY[1]

1. *School of Biological and Marine Sciences, Plymouth University, Drake Circus, PL4 8AA, Plymouth, UK. jak.mccarroll@plymouth.ac.uk.*
2. *School of Geography and Planning, University of Liverpool, Brownlow Hill, Liverpool, UK.*

Abstract: Gravel beach morphologic change is a function of combined cross- and alongshore transport. At present, numerical methods deal with these processes separately. We present observations from Start Bay, UK, of extreme storm response and recovery, across five gravel sub-embayments (lengths 250 m to 5 km). An easterly storm sequence in Feb-Mar 2018 forced massive alongshore transport (rotation and headland bypassing) and cross-shore transport including erosion of the barrier, destruction of barrier-crest roads, and distribution of material offshore. We demonstrate that profile response is a function of embayment length and headland proximity, such that: (i) pocket embayments (~250 m) experience a uniform response; (ii) short embayments (~500 m) rotate around a pivot point; (iii) longer bays (>1 km), exhibit a weak cut-fill response near the mid-point; and (v) long beaches (>5 km) show a strong cross-shore response, with rotation near the headlands. This study aids development of fully-coupled gravel transport models.

Introduction

Gravel beaches are a common occurrence across the higher latitudes and the capacity to predict morphologic change on gravel beaches is necessary for effective coastal management of this type of coastline. Gravel transport within an embayment may occur in the longshore direction due to variations in alongshore wave power, resulting in beach rotation (Wiggins et al., 2019), while cross-shore transport during storms (McCall et al., 2015) may occur as erosion from the upper beach and deposition in the sub-tidal (cut-fill) or as barrier rollover. It is typical for these effects to combine, e.g., a storm from a given direction may rapidly deplete the sediment downdrift of a headland, allowing subsequent wave action to damage coastal infrastructure on or behind the crest of the barrier (Chadwick et al., 2005).

Current process-based numerical models applied to gravel beaches can accurately predict hydrodynamic activity such as overtopping (XBeach-G; McCall et al., 2014) and 1D morphodynamics for storm conditions (McCall et al., 2015). Bergillos et al., (2017) effectively coupled XBeach-G with a parametric longshore transport equation to predict combined cross- and longshore transport on a mixed sand-gravel beach for an open stretch of coastline (absent headlands), providing a transitional step to a fully coupled 2D-horizontal gravel morphodynamic model. Further observations of gravel transport will assist in developing such a broadly applicable predictive model, with observations around headlands and on embayments of varying length being particularly important, as these controls are likely to have a pronounced effect on cross- and alongshore transport processes (Vieira da Silva et al., 2016).

Our objective is to examine profile response, across an extreme storm and subsequent recovery period, for five gravel embayments of varying length (250 m to 5.4 km). We define profile response as alongshore dominant (rotation) or cross-shore dominant (cut-fill), then test if there is a relationship between type of profile change, beach length and proximity of a profile to the nearest headland. A separate effort (McCarroll et al., 2019) examines alongshore flux rates and headland bypassing rates for the same storm event described here.

Site Description

Start Bay, Devon, UK (Fig. 1) is a SE facing embayment with a 12 km shoreline, comprised of rocky stretches and five sub-embayments. From south to north these include: Hallsands (HS; 250 m long), Beesands (BS; 1.5 km), Slapton Sands (SS; 5.4 km), Forest Cove (FC; 1 km) and Blackpool Sands (BK; 650 m). Sediment is fine gravel (range: 2-50 mm, D_{50} = 5 mm; Chadwick et al., 2005), tidal regime is macrotidal with 4.3 m spring tidal range. Waves are generally low to moderate (mean significant wave height, H_s = 0.7 m), with a bi-modal storm climate of southerly and easterly storms (H_s > 2.2 m) commonly occurring (Fig. 1b). The site is heavily researched (e.g., Ruiz de Alegria Arzaburu and Masselink, 2010; Wiggins et al., 2019), with significant beach rotation and headland bypassing known to occur due to variations in the bi-modal storm regime.

Methods

A field campaign measuring hydrodynamic activity and morphologic change across Start Bay was conducted from Jan-May 2018. Components of this dataset presented here include: (i) topo-bathymetric profile surveys conducted along the length of the embayment; and (ii) directional wave buoy data (Fig. 1c-h), provided by the Channel Coastal Observatory. During the measurement period, an extended easterly storm sequence occurred (22 Feb – 2 Mar, Fig. 1e-g), culminating in the named storm 'Emma' (1-2 Mar). Extreme value analysis indicates this was a 1-in-50-year event which caused widespread damage across Start Bay, including destruction of roads on the BS and SS barriers (Fig. 1i-k). Wave heights at the buoy peaked at H_s = 5.6 m (Fig. 1e). Cumulative alongshore wave power (P_y; Fig. 1h) was calculated using the method for wave transformation and breaking given in Van Rijn, (2014), determined for a point onshore of the wave buoy (profile SS16).

Topographic survey data were collected with walked real-time-kinematic Global Position System (RTK-GPS) profile surveys. Bathymetric survey data was obtained from a vessel with a coupled single-beam echosounder and RTK-GPS at 1 Hz. Combined topo-bathymetric profiles were taken within 1-week preceding and following the storm event, with an additional topo-bathymetric survey conducted in early May 2018, to observe the initial stages of recovery. Some profiles did not have pre-storm bathymetric surveys conducted and linear interpolation from adjacent profiles was used to estimate sub-tidal volume. Full methods are provided in McCarroll et al. (2019). Profile volume change (in m^3/m alongshore) was calculated for two time periods (storm: 21/2 – 2/3/2018; and recovery: 3/3 – 9/5/2018). Volume change was determined for the subtidal ($\Delta V_{subtidal}$; below -2 m Ordnance Datum Newlyn [ODN]) and for the sub-aerial ($\Delta V_{sub\text{-}aerial}$; above 2 m ODN). Volume change is described in terms of *net change* ($\Delta V_{net} = \Delta V_{subtidal} + \Delta V_{sub\text{-}aerial}$), which trends to 0 if no alongshore flux gradient is present, and *gross change* ($\Delta V_{gross} = |\Delta V_{subtidal}| + |\Delta V_{sub\text{-}aerial}|$), where vertical bars are absolute values.

We introduce two simple parameters to classify profile change in terms of cross- and alongshore factors. Note that 'rotation' always refers to beach rotation related to alongshore flux. First, profile volume change type ($\Delta V_{type} = \Delta V_{net} / \Delta V_{gross}$) distinguishes rotational profile response from a cross-shore cut-fill response. For ΔV_{type} = -1, both subtidal and sub-aerial regions erode ($\Delta V_{net} = -\Delta V_{gross}$; indicates dominance of 'erosional rotation'). For ($-1 < \Delta V_{type} < 0$), the sub-aerial and sub-tidal have opposite sign, indicating a dominant cross-shore cut-fill response, but net change is erosional ($\Delta V_{net} < 0$). $\Delta V_{type} = 0$ indicates cut-fill with no net change. Next, ($0 < \Delta V_{type} < 1$) is a cut-fill response, but with net accretion. Last, for $\Delta V_{type} = 1$, both upper and lower regions accrete ('accretional rotation'). Note that ΔV_{type} does not address alongshore volume flux, only the resultant profile expression, nor does it address the direction of cross-shore transport (off- or onshore).

The second parameter, $\Delta V_{x\text{-}mag}$ (m^3/m) = $\Delta V_{gross} - |\Delta V_{net}|$, addresses the magnitude of the cross-shore response. $\Delta V_{x\text{-}mag} = 0$ indicates a rotation dominant response (i.e., $\Delta V_{gross} = |\Delta V_{net}|$), while large $\Delta V_{x\text{-}mag}$ indicates a strong cross-shore response. Note that $\Delta V_{x\text{-}mag}$ has not been normalized to account for alongshore wave power variations.

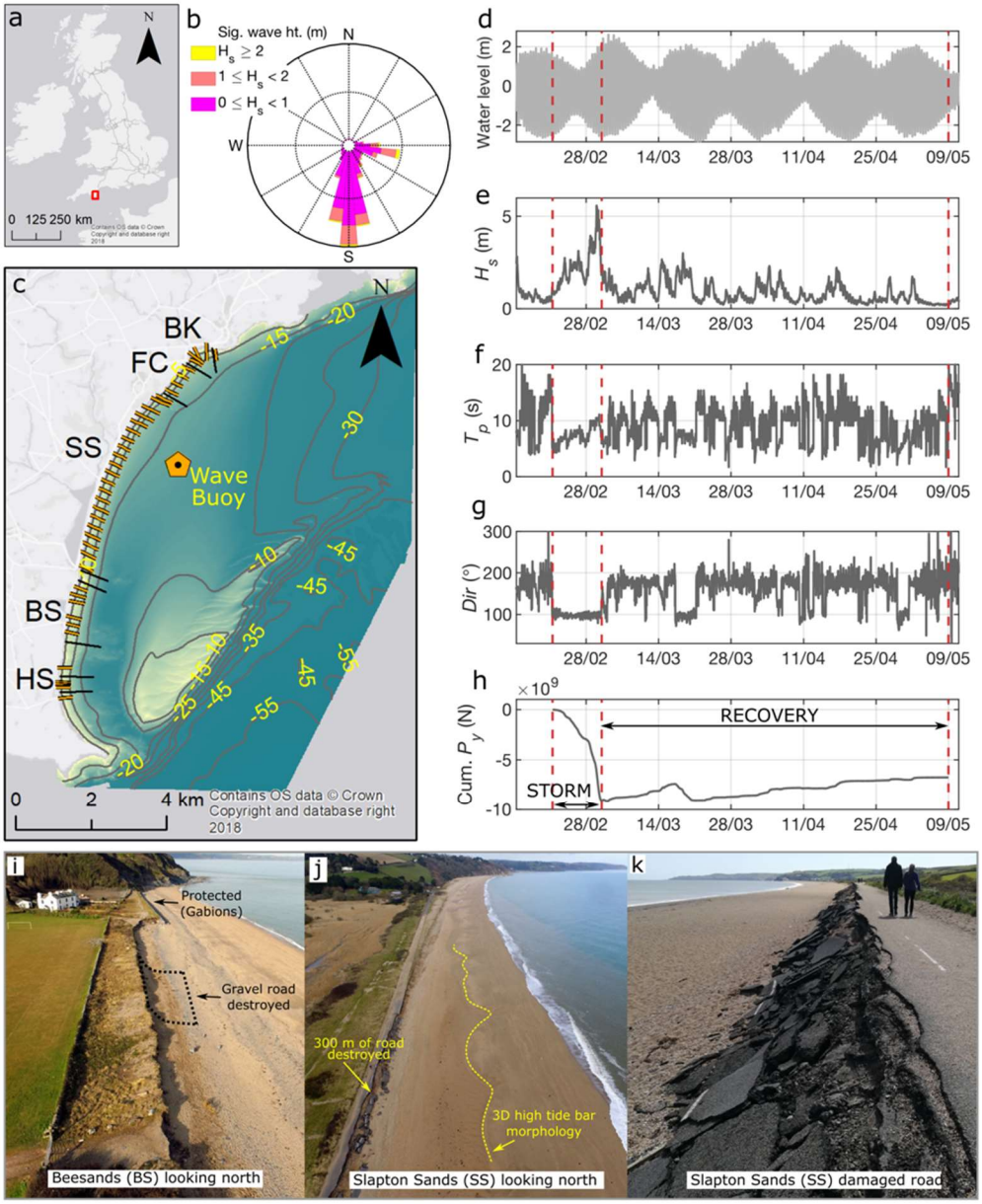

Fig. 1. Start Bay site and wave data, including: (a) site location; (b) wave rose for buoy data [2007-2018]; (c) site map with wave buoy and profile locations indicated; (d) water level timeseries [FOAM-AMM7, http://marine.copernicus.eu]; (e-g) time series of wave height, peak period and direction from wave buoy; (h) cumulative alongshore wave power [P_y]; and (i-k) photos of storm damage (photos: Peter Ganderton).

Results

Volume changes across Start Bay for the storm and recovery periods are presented in Figure 2. The easterly wave sequence generated southward sediment flux and extreme volumetric profile changes with the greatest magnitudes toward the north (right of Fig. 2). Profile response near headlands was characterized by large sub-aerial and subtidal accretion updrift of headlands (e.g., BK1, Fig. 2b, +400 m^3/m) and corresponding full-profile erosion downdrift of headlands (e.g., SS19, -400 m^3/m). Shorter embayments rotated around a pivot point near

the center of the embayment (e.g., BK, Fig. 2b), with the full profile (sub-aerial and subtidal) both accreting or eroding. The longest embayment (SS) was characterized by an extensive region of sub-aerial erosion and subtidal accretion (4500 m to 7600 m, SS, Fig. 2b), indicating a dominant cut-fill response (net cross-shore erosion).

The recovery period (Fig. 2c) involved gradual northward directed transport with cumulative northward longshore wave power equivalent to approx. one third the magnitude of the storm period (Fig. 1h). Volumetric changes were generally the inverse of the storm period, though of lower magnitude. Again, the shorter embayments (BK, FC) rotated around a pivot point, while the middle sections of the longer embayments exhibited subtidal erosion and sub-aerial accretion (net onshore transport).

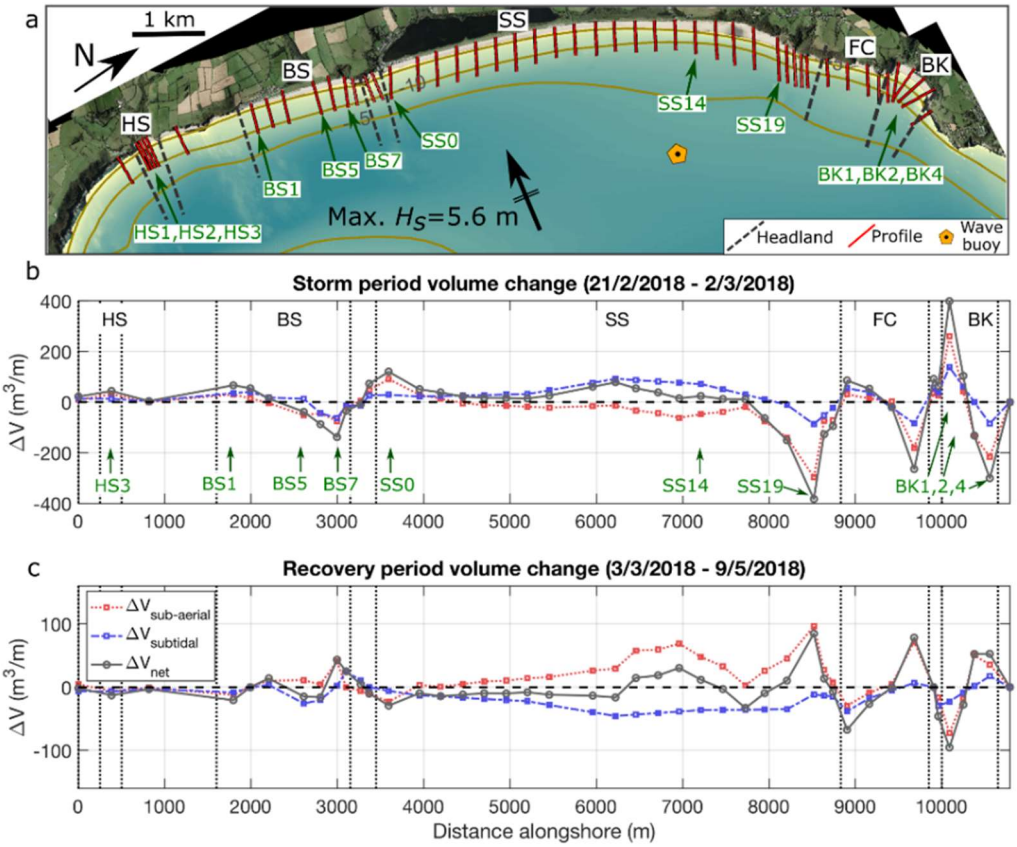

Fig. 2. Profile volume change, with: (a) profile map; (b) storm period; and (c) recovery period. Profiles shown in Fig. 3 are annotated in green. Note differing y-axis in (b) and (c).

Selected profiles are now examined in detail across four of the sub-embayments (Fig. 3). At the shortest ('pocket') embayment (HS, 250 m, Fig. 3-top row), all profiles accreted during the storm period (i.e., no rotation), though this may be in part due to a more shore-normal wave angle (Fig. 2a). By contrast, the 650 m long BK embayment displayed a massive rotational response over the storm period near the headlands (Fig. 3, BK1, BK4), with minimal change near the mid-point (BK2). At the 1.5 km long BS embayment, rotation was dominant near the headlands (Fig. 3, BS1, BS7) though a subtle cross-shore cut-fill response was apparent near the center of the beach (BS5). For the longest embayment (SS, 5.4 km, Fig. 3-bottom row), an extreme cross-shore response is evident at the middle of the embayment (SS14), with net offshore transport and 3D high tide bar morphology

(Fig. 1j).

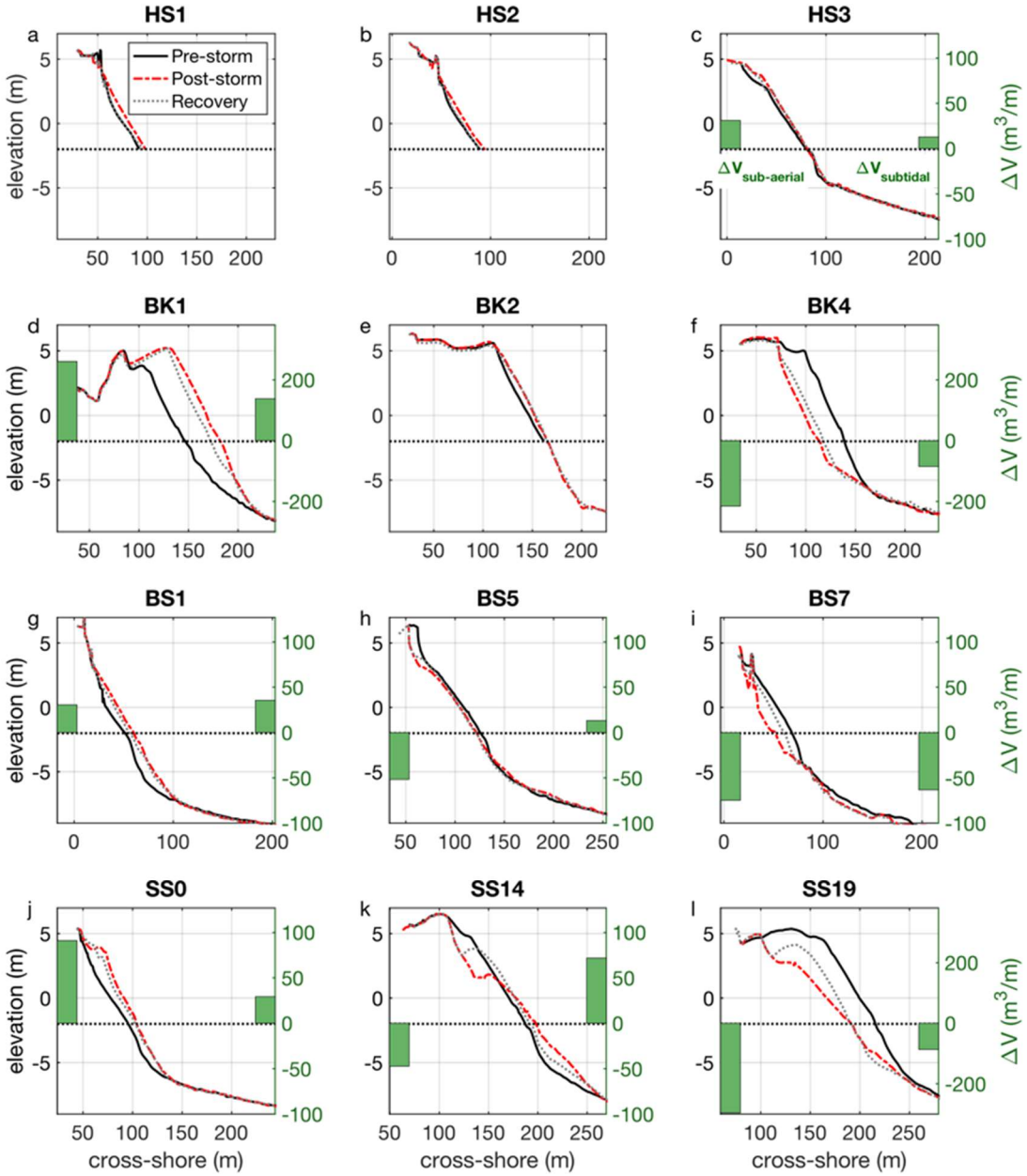

Fig. 3. Profile response with profile locations indicated in (Fig. 2a). Lines indicate profiles (left axes). Green bars (right axes) are volume change over the storm period for the sub-aerial (left bar) and subtidal (right bar). Volume change bars are not included for profiles lacking subtidal surveys [a, b, e] and are not shown for the recovery period. Note right axes use different scales.

Discussion

Our objective was to test for a relationship between type of profile change (alongshore rotation dominant or cross-shore cut-fill dominant) as a function of beach length and profile location relative to the headlands. The results (Figs. 2,3) suggest that as beach length increases, the extent of shoreline exhibiting a cross-shore dominant response increases. We now seek to quantify and interpret this relationship using the parameters ($\Delta V_{type} = \Delta V_{net} / \Delta V_{gross}$) and ($\Delta V_{x\text{-}mag} = \Delta V_{gross} - |\Delta V_{net}|$). Figure 4 presents the alongshore variation in ΔV_{type} for each of the sub-embayments. Over the storm period, the alongshore extent of each embayment with a cross-shore dominant response ($-1 < \Delta V_{type} < 1$) increases with embayment length (Fig. 4, pink shading), as does the maximum magnitude of cross-shore response (max[$\Delta V_{x\text{-}mag}$], left side of Fig. 4).

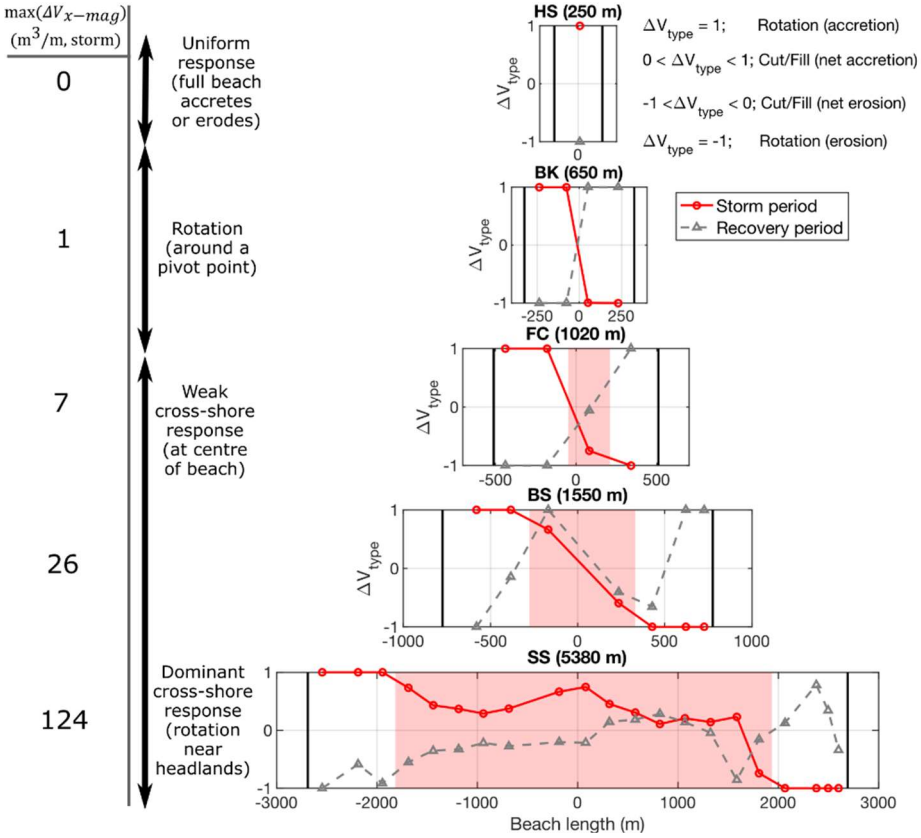

Fig. 4. Alongshore variation of (ΔV_{type}) for the five sub-embayments of Start Bay (panels HS, BK, FC, BS, SS). Maximum cross-shore response (max[$\Delta V_{x\text{-}mag}$]) for each embayment during the storm period is indicated in the left column.

The variations in profile response type (ΔV_{type}) and magnitude of cross-shore response ($\Delta V_{x\text{-}mag}$) are now synthesized (Fig. 5). First, the ratio of cut-fill response (extent of pink shading in Fig. 4) is compared against beach length (Fig. 5a), with a clear positive relationship apparent, grading from an alongshore uniform response (HS), through pure rotation (BK), to a cross-shore response along most of the shoreline (SS). A similar relationship is observed over the recovery period (Fig. 5a, grey-dashed line). Second, the maximum cross-shore response for each embayment is compared to embayment length (Fig. 5b). Again, a clear positive relationship is evident,

across both the storm and recovery periods. These results demonstrate that as beach length increases, that both the alongshore extent and magnitude of a cross-shore dominant response increases.

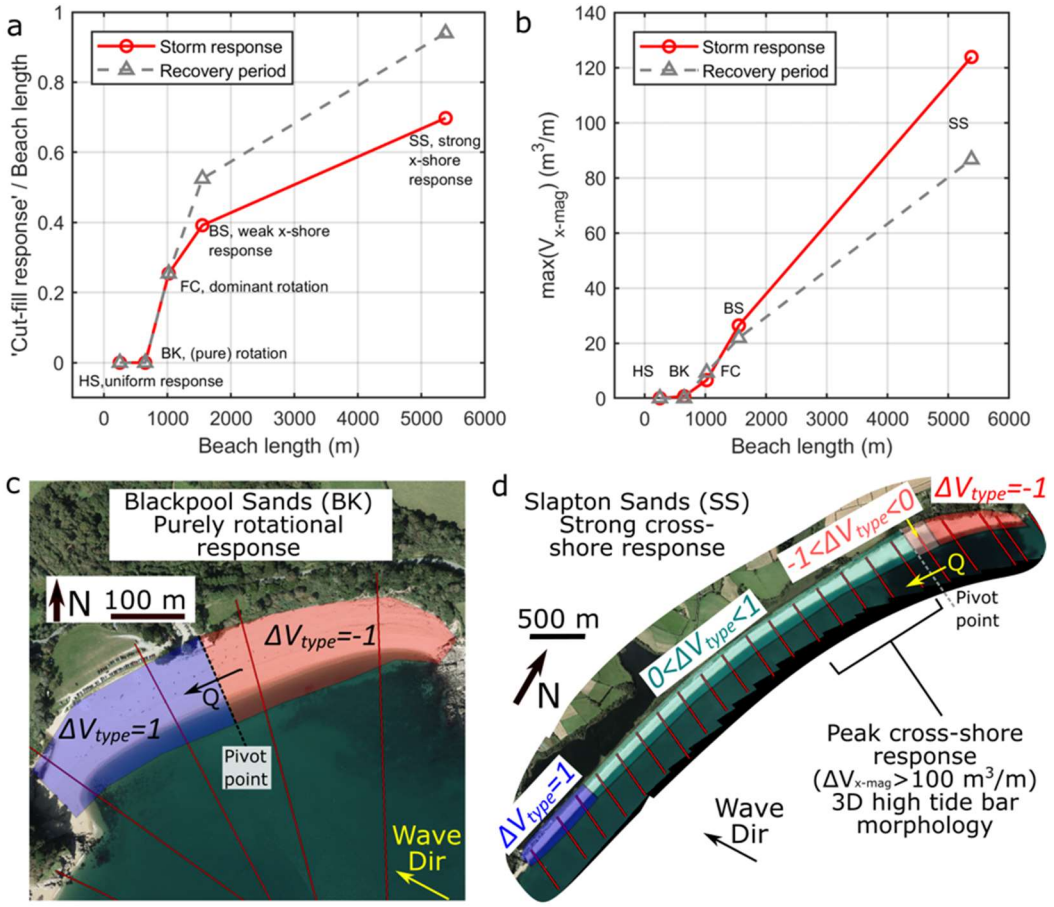

Fig. 5. Profile response type and magnitude as a function of embayment length and headland proximity. (a) Ratio of cut-fill response (-1 < ΔV_{type} < 1) to embayment length; (b) [max($\Delta V_{x\text{-}mag}$)] against embayment length; (c) schematic rotational response of Blackpool Sands; and (d) cross-shore dominant response for Slapton Sands. 'Q' indicates sediment flux.

Two end-member scenarios are presented, combining conceptual interpretation with observations. These include a 'purely rotational response' (Fig. 5c, BK) and a more complex response for a long embayment (Fig. 5d, SS), with rotation near the headlands and extensive cross-shore dominant transport along the middle of the beach.

The storm response observed along the middle of the SS embayment included development of 3D high tide bar morphology, characterized by a ridge backed by a flat trough around the mean high tide level (Fig. 1j, Fig. 3k). This response is consistent with previous observations at this site (Ruiz de Alegria-Arzaburu and Masselink, 2010), where easterly storms caused supratidal erosion, intertidal accretion and overall volume gain. Additionally, this beach state has been observed at other locations (Poate et al., 2015, Bergillos et al., 2017) and has been successfully modelled with XBeach-G (Bergillos et al., 2017). However, this beach state / storm response is not clearly included with conceptual models of gravel beach dynamics (McCall et al., 2015), contrasting with suggestions that bars do not occur on gravel beaches (Buscombe and Masselink, 2006).

A next-step in cross- and alongshore modelling of gravel beaches will be to take the approach of Bergillos et al. (2017) and introduce headlands. This paper provides a conceptual template for the relationship between embayment length and cross-shore response when calibrating such a model.

An important caveat is that the 'embayment length and cross-shore response type' relationship may not hold over longer time periods. Wiggins et al. (2019) examined the annual response of the field site described here (Start Bay, UK) over several multi-year epochs and did not observe the correlation between cross-shore response, embayment length and headland proximity. In contrast, Wiggins et al., (2019) observed a 'purely rotational' response across all embayments (including the 5.4 km SS). This suggests that over intermediate time periods (months), cross-shore processes on gravel beaches relatively quickly return sediment onshore, as opposed to sandy beaches where this may take years (Scott et al., 2016). Therefore, we suggest the relationships we have identified (Figs. 4,5) are valid only for storm response and the immediate recovery. This is consistent with the idea of morphodynamic turbulence (Lazarus et al., 2019), where event scale variability is not indicative of long-term trends in shoreline change.

Conclusions

An extreme storm sequence and 2-month recovery period were observed across five adjacent gravel embayments. These observations were used to demonstrate that cross-shore profile response was a function of beach length and headland proximity, categorizing response as dominantly alongshore (rotation) or cross-shore (cut-fill). This suggests a continuum of gravel beach response relative to beach length, when both cross- and alongshore transport processes are significant, such that: (i) for 'pocket' embayments [<-250 m] response is near-uniform alongshore; (ii) for short embayments [~500 m], a purely rotational response around a pivot point occurs; (iii) at ~1 km length, a weak cross-shore response emerges around the beach mid-point; and (iv) for long embayments [>5 km] a strong cross-shore response dominates the bulk of the shoreline extent, with rotation dominance occurring only adjacent to the headlands. These results will be used to aid in the development of process based and empirical gravel beach morphodynamic numerical models.

Acknowledgements

This work was funded by UK Natural Environment Research Council grant (NE/M004996/1; BLUE-coast project). We thank all those who assisted with the field work, in particular: Nieves Valiente, Peter Ganderton, Aaron Barrett and Tim Poate. Directional wave buoy data were provided by the Channel Coastal Observatory.

References

Bergillos, R. J., Masselink, G., and Ortega-Sánchez, M. (2017). "Coupling cross-shore and longshore sediment transport to model storm response along a mixed sand-gravel coast under varying wave directions," *Coastal Engineering*, *129*, 93-104.

Buscombe, D., and Masselink, G. (2006). "Concepts in gravel beach dynamics," *Earth-Science Reviews*, *79*(1-2), 33-52.

Chadwick, A. J., Karunarathna, H., Gehrels, W. R., Massey, A. C., O'Brien, D., and Dales, D. (2005). "A new analysis of the Slapton barrier beach system, UK," *Proceedings of the Institution of Civil Engineers-Maritime Engineering*, Thomas Telford Ltd., 158(4), 147-161.

Lazarus, E. D., Harley, M. D., Blenkinsopp, C. E., and Turner, I. L. (2019). "Environmental signal shredding on sandy coastlines," *Earth Surface Dynamics*, *7*(1), 77-86.

McCall, R. T., Masselink, G., Poate, T. G., Roelvink, J. A., Almeida, L. P., Davidson, M., and Russell, P. E. (2014). "Modelling storm hydrodynamics on gravel beaches with XBeach-G," *Coastal Engineering*, *91*, 231-250.

McCall, R. T., Masselink, G., Poate, T. G., Roelvink, J. A., and Almeida, L. P. (2015). "Modelling the morphodynamics of gravel beaches during storms with XBeach-G," *Coastal Engineering*, *103*, 52-66.

McCarroll, R. J., Masselink, G., Wiggins, M., Scott, T., Billson, O., and Conley, D.C. (2019). "Gravel transport at half the rate of sand? Longshore transport and headland bypassing during an extreme event," *Geophysical Research Letters*, (under review).

Poate, T., Masselink, G., McCall, R., Russell, P., and Davidson, M. (2015). "UK storms 2014: gravel beach response," *The Proceedings of the Coastal Sediments 2015*.

Ruiz de Alegria-Arzaburu, A., and Masselink, G. (2010). "Storm response and beach rotation on a gravel beach, Slapton Sands, UK," *Marine Geology*, *278*(1-4), 77-99.

Scott, T., Masselink, G., O'Hare, T., Saulter, A., Poate, T., Russell, P., Davidson, M., and Conley, D. (2016). "The extreme 2013/2014 winter storms: Beach recovery along the southwest coast of England," *Marine Geology*, 382, 224-241.

Van Rijn, L. C. (2014). "A simple general expression for longshore transport of sand, gravel and shingle," *Coastal Engineering*, *90*, 23-39.

Vieira da Silva, G., Toldo Jr, E. E., Klein, A. H. D. F., Short, A. D., and Woodroffe, C. D. (2016). "Headland sand bypassing—Quantification of net sediment transport in embayed beaches, Santa Catarina Island North Shore, Southern Brazil," *Marine Geology*, *379*, 13-27.

Wiggins, M., Scott, T., Masselink, G., Russell, P., and McCarroll, R. J. (2019). "Coastal embayment rotation: Response to extreme events and climate control, using full embayment surveys," *Geomorphology*, *327*, 385-403.